JOURNAL OF GEOPHYSICAL RESEARCH, VOL. 113, D17310, doi:10.1029/2008JD009803, 2008

The North American Mercury Model Intercomparison Study (NAMMIS): Study description and model-to-model comparisons

O. Russell Bullock Jr.,[1] Dwight Atkinson,[2] Thomas Braverman,[3] Kevin Civerolo,[4] Ashu Dastoor,[5] Didier Davignon,[5] Jia-Yeong Ku,[4] Kristen Lohman,[6] Thomas C. Myers,[7] Rokjin J. Park,[8,10] Christian Seigneur,[6] Noelle E. Selin,[9,10] Gopal Sistla,[4] and Krish Vijayaraghavan[6]

Received 8 January 2008; revised 15 May 2008; accepted 18 June 2008; published 9 September 2008.

[1] An atmospheric mercury model intercomparison study has been conducted to compare three regional-scale atmospheric mercury models, CMAQ, REMSAD, and TEAM, in a tightly constrained testing environment with a focus on North America. Each of these models used the same horizontal modeling grid, pollutant emission information, modeled meteorology, and boundary conditions to the greatest extent practical. Three global-scale atmospheric mercury models were applied to define three separate initial condition and boundary condition (IC/BC) data sets for elemental mercury, reactive gaseous mercury, and particulate mercury air concentrations for use by the regional-scale models. The monthly average boundary concentrations of some mercury species simulated by the global models were found to vary by more than a factor of 10, especially at high altitudes. CMAQ, REMSAD, and TEAM were each applied three times, once for each IC/BC data set, to simulate atmospheric mercury transport and deposition during 2001. This paper describes the study design and shows qualitative model-to-model comparisons of simulation results on an annual basis. The air concentration patterns for mercury simulated by the regional-scale models showed significant differences even when the same IC/BC data set was used. Simulated wet deposition of mercury was strongly influenced by the shared precipitation data, but differences of over 50% were still apparent. Simulated dry deposition of mercury was found to vary between the regional-scale models by nearly a factor of 10 in some locations. Further analysis is underway to perform statistical comparisons of simulated and observed mercury wet deposition using weekly and annual sample integration periods.

Citation: Bullock, O. R., Jr., et al. (2008), The North American Mercury Model Intercomparison Study (NAMMIS): Study description and model-to-model comparisons, *J. Geophys. Res.*, *113*, D17310, doi:10.1029/2008JD009803.

1. Introduction

[2] Air quality simulation models have been used to estimate source attribution for observed mercury (Hg) deposition to the United States [*US EPA*, 2005a; *Seigneur et al.*, 2004] and to various nations in Europe [*Ryaboshapko et al.*, 2007a]. These model simulations have, in some cases, led to rather different conclusions for reasons that remain unclear. An atmospheric Hg model inter-comparison study was previously conducted by the Meteorological Synthesizing Centre – East (MSC-East) with the participation of various models from Europe and North America [*Ryaboshapko et al.*, 2002, 2007a, 2007b]. This study focused on modeling atmospheric Hg over Europe. It provided valuable information about the way the models defined the concentration of pollutants at their boundaries, defined meteorology, and treated specific physical and chemical processes affecting Hg and other relevant substances. It also showed that these differing modeling assumptions and process treatments can lead to significantly different modeling results. However, it

[1]National Exposure Research Laboratory, U.S. Environmental Protection Agency, Research Triangle Park, North Carolina, USA.
[2]Office of Water, U.S. Environmental Protection Agency, Washington, DC, USA.
[3]Office of Air Quality Planning and Standards, U.S. Environmental Protection Agency, Research Triangle Park, North Carolina, USA.
[4]Division of Air Resources, New York State Department of Environmental Conservation, Albany, New York, USA.
[5]Air Quality Research Division, Environment Canada, Dorval, Quebec, Canada.
[6]Air Quality Division, Atmospheric and Environmental Research, Inc., San Ramon, California, USA.
[7]ICF International, San Rafael, California, USA.
[8]School of Earth and Environmental Sciences, Seoul National University, Seoul, South Korea.
[9]Massachusetts Institute of Technology, Department of Earth, Atmospheric and Planetary Sciences, Cambridge, Massachusetts, USA.
[10]Formerly at Department of Earth and Planetary Sciences, Harvard University, Cambridge, Massachusetts, USA.

0148-0227/08/2008JD009803$09.00

was not able to determine if differences in the simulated Hg air concentration and deposition were due mostly to differences in model input data or differences in the way important atmospheric processes were treated in each model.

[3] The North American Mercury Model Intercomparison Study (NAMMIS) is a follow-on effort to apply regional-scale atmospheric Hg models in a more tightly constrained testing environment, this time with a focus on North America where standardized measurement of Hg wet deposition has been underway since the mid-1990s. With each regional-scale model using the same input data sets for initial conditions, meteorology, emissions and boundary concentration values, and applied to the same horizontal modeling domain, the effects of input data and scientific process treatments can be decoupled and better understood so that guidance can be provided to the research community regarding which scientific process uncertainties are contributing most to observed discrepancies in model simulations of Hg deposition.

2. Study Design

[4] The NAMMIS participants include governmental, academic and private research organizations, namely the U.S. Department of Commerce's National Oceanic and Atmospheric Administration (NOAA), U.S. Environmental Protection Agency (EPA), Environment Canada (EC), the New York State Department of Environmental Conservation (NYSDEC), Atmospheric and Environmental Research, Inc. (AER), Harvard University, and ICF International (ICFI). Three regional-scale atmospheric Hg models are the prime subjects of the study: the Community Multi-scale Air Quality model (CMAQ) developed by NOAA and EPA, the Regional Modeling System for Aerosols and Deposition (REMSAD) developed by ICFI, and the Trace Element Analysis Model (TEAM) developed by AER. Descriptions of these three regional-scale models are provided in section 3.

[5] CMAQ, REMSAD and TEAM were each applied to simulate the entire year of 2001 three times, each time using a different initial condition and boundary condition (IC/BC) data set developed from one of three global-scale models: the Chemical Transport Model for Hg (CTM-Hg) from AER, the GEOS-Chem model from Harvard University, and the Global/Regional Atmospheric Heavy Metals (GRAHM) model from EC. These global-scale models are not the primary subjects of this study, but they did exhibit some interesting and useful differences in their simulation results as described in section 4. All three regional-scale models were applied using the same inputs for emissions and meteorology to the greatest practical degree. All regional-scale modeling results were sent to NYSDEC for inter-comparison analysis and for comparison to observed data from the Mercury Deposition Network (MDN) [*Vermette et al.*, 1995] and special event-based monitoring at the Proctor Maple Research Center (PMRC) near Underhill, VT [*Keeler et al.*, 2005]. Model results inter-comparison is described in this paper. Comparison of model simulations to observations is underway and the results will be reported in a future publication.

3. Description of the Regional-Scale Models

[6] All regional-scale atmospheric Hg models used in this study simulate three basic Hg species: elemental mercury (Hg^0), reactive gaseous mercury (RGM), and particulate mercury (PHg). RGM is a commonly used operational term to describe gaseous forms of Hg that are more water-soluble and chemically reactive than the elemental form. Its exact composition remains largely unknown because currently available monitoring technology cannot yet quantify specific Hg compounds at ambient air concentrations. RGM is known to be comprised almost entirely of divalent mercury (Hg^{2+}) since Hg compounds at other valence states tend to be chemically unstable in the atmosphere. The same is true regarding PHg, except that Hg^0 could also be a constituent since it is known to bind to certain aerosol materials (e.g., activated carbon). CMAQ, REMSAD and TEAM all use an Eulerian-type modeling framework and are commonly referred to as "fixed-grid" models. All three of the regional-scale models utilized the same 36-km horizontal grid system based on a Lambert conformal map projection with 148 (west-to-east) by 112 (south-to-north) grid cells covering most of North America. CMAQ and REMSAD used the exact same vertical coordinate system, but as described below, TEAM's coordinate system was slightly different. Basic characteristics of all three regional-scale models are summarized in Table 1.

3.1. CMAQ Model

[7] The CMAQ modeling system is a comprehensive air quality model designed to operate on a range of domain sizes from urban to continental [*Byun and Schere*, 2006]. CMAQ reflects the state-of-the-science in addressing the atmospheric processes critical for simulating non-linear photochemistry and the reaction products associated with the transformation and deposition of Hg. A test version of the CMAQ model was first adapted for Hg simulation by adding various gaseous and aqueous chemical reactions involving Hg and by also adding molecular chlorine gas to the model [*Bullock and Brehme*, 2002]. To support the U.S. EPA's Clean Air Mercury Rule (CAMR), these same Hg adaptations were added to CMAQ version 4.3 employing the CB-IV gas-phase chemistry mechanism described by *Gery et al.* [1989] along with other updates to improve the underlying science and address comments from peer review [*US EPA*, 2005a]. These updates include: (1) the gaseous Hg^0 reaction with H_2O_2 assumes the formation of RGM rather than PHg, (2) the gaseous Hg^0 reaction with ozone assumes the formation of 50% RGM and 50% PHg rather than 100% PHg, (3) the gaseous Hg^0 reaction with OH assumes the formation of 50% RGM and 50% PHg rather than 100% PHg, and (4) the kinetic rate constant for the gaseous Hg^0 + OH reaction was lowered slightly to 7.7×10^{-14} cm^3 $molecules^{-1}$ s^{-1}. This updated version of the CMAQ Hg model was also applied for the NAMMIS.

[8] CMAQ requires a variety of input files that contain information pertaining to the modeling domain and simulation period. These include hourly emissions estimates and meteorological data in every grid cell as well as a set of pollutant concentrations to initialize the model and to specify concentrations along the boundaries of the modeling domain.

[9] Key science options for the CMAQ are documented on the Community Modeling and Analysis System (CMAS) web site (http://www.cmascenter.org). These model science options were applied for the NAMMIS as

Table 1. Characteristics of the Regional Models as Applied for the NAMMIS

Model Name	CMAQ	REMSAD	TEAM
Horizontal resolution (km)	36 × 36	36 × 36	36 × 36
Model top	10 kPa	10 kPa	14,183 m
Number of layers	14	14	14
Vertical coordinates	sigma-pressure (σ_p)	sigma-pressure (σ_p)	geometric height above ground level
Terrain	grid resolved	grid resolved	none
Turbulent diffusion			
Horizontal	K-theory	K-theory	none
Vertical	K-theory	K-theory	K-theory
Non-Hg gaseous chemistry	CB-IV	CB-V	non-Hg species input from GEOS-Chem
Dry deposition			
Hg^0	none[a]	none	not reported[b]
RGM	resistance approach	resistance approach	resistance approach
PHg	resistance approach	resistance approach	resistance approach
Re-emission of Hg^0	none[a]	*Syrakov* [2001]	1/2 of total deposition
Wet deposition	cloud microphysics	solution scavenging	cloud microphysics
Gaseous oxidation agents for Hg	O_3, Cl_2, H_2O_2, OH	O_3, H_2O_2, OH	O_3, H_2O_2, OH, HCl,Cl_2
Aqueous oxidation agents for Hg	O_3, OH, Cl^-	O_3, OH, Cl^-	O_3, OH
Aqueous reduction agents for Hg	$SO_3^=$, HO_2, hν[c]	$SO_3^=$, HO_2	$SO_3^=$, HO_2

[a]Dry deposition of Hg^0 is assumed to be neutralized by its re-emission flux.
[b]Dry deposition of Hg^0 is simulated in TEAM using a resistance approach but not routinely reported because most of it is assumed to be emitted back to the atmosphere.
[c]Photo-reduction of $Hg(OH)_2$ to Hg^0 is treated, but the kinetic rate currently applied yields no significant effect.

follows. The CB-IV gas-phase chemical mechanism [*Gery et al.*, 1989] was solved using the Euler Backward Iterative (EBI) scheme. Advection of all pollutant species was calculated using the Piecewise Parabolic Method (PPM). Vertical diffusion was calculated using K-theory eddy diffusivity (1 m^2/sec minimum). Dry deposition was solved with the M3DRY module using the Pleim-Xiu land surface model [*Xiu and Pleim*, 2001; *Pleim and Xiu*, 2003]. Dry deposition of gaseous Hg^0 was not explicitly simulated. The natural and recycled Hg^0 emission fields defined from input data were assumed to be net flux values where opposing dry deposition forces are already taken into account. Aqueous chemistry was calculated using a RADM bulk scheme incorporated in a special mercury version of the AQCHEM subroutine.

[10] The CMAQ modeling was performed with 36-km horizontal grid cell sizes and 14 vertical layers defined between the surface and the 100-mb pressure level in the model's terrain-following sigma-pressure (σ_P) vertical coordinate system with the following layer boundaries: σ_P = 1.0, 0.995, 0.99, 0.98, 0.96, 0.94, 0.91, 0.86, 0.8, 0.74, 0.65, 0.55, 0.4, 0.2, and 0. These layers were chosen to fit in a modular fashion into the MM5's 34-layer structure, which was defined on the same σ_P coordinate boundaries.

3.2. REMSAD Model

[11] Version 8 of the Regional Modeling System for Aerosols and Deposition (REMSAD) was used for this modeling analysis. REMSAD is a three-dimensional Eulerian grid model that provides estimates of the concentrations and deposition (both wet and dry) of the simulated pollutants at each grid location in the modeling domain [*ICF*, 2005]. REMSAD utilized a terrain following, σ_P coordinate system with σ_P levels defined identically to those in the CMAQ grid system.

[12] REMSAD uses the advection scheme proposed by *Smolarkiewicz* [1983]. Turbulent diffusion is treated using K-theory. Vertical turbulent exchange coefficients were prepared during the processing of the MM5 output files and were provided to REMSAD as an input file. Wet deposition of gas phase species is treated according to their solubility in rain and cloud water, based on the work of *Hales and Sutter* [1973]. Wet deposition of aerosols in REMSAD utilizes many of the relationships established by *Scott* [1978], which relate rainfall rate and cloud type to fraction of ambient sulfate within rainwater reaching the ground. The equations have been expanded from sulfate only to treat any aerosol species.

[13] The dry deposition algorithm used in REMSAD uses deposition velocities for each species that are calculated as a series of resistance terms according to the methodology developed for RADM [*Wesely*, 1989]. Dry deposition of elemental mercury is not calculated by REMSAD.

[14] Gas phase chemistry is treated using the Carbon Bond mechanism version 5 (CB-V) as described in *SAI* [2002]. The CB-V photochemical mechanism is an expanded version of CB-IV [*Gery et al.*, 1989]. The principal enhancement in CB-V relative to CB-IV is the explicit treatment of acetaldehyde rather than including it in higher aldehydes. The CB-V mechanism is derived from the mechanism implemented in UAM-V [*SAI*, 1999] with some specific adaptations for REMSAD. These adaptations include separating the biogenic hydrocarbon species from anthropogenic hydrocarbons (by carrying isoprene and terpenes explicitly) and allowing for the production of semi-volatile hydrocarbon compounds that lead to the formation of secondary organic aerosols (SOA).

[15] The chemical transformations of mercury included in REMSAD are based on the review of current status of atmospheric chemistry of mercury presented by *Lin and Pehkonen* [1999] with a number of updates based on more recent literature. The reactions and products in REMSAD are very similar to CMAQ, but it parameterizes the adsorption of Hg^{2+} to soot rather than solving it explicitly.

REMSAD does not carry chlorine as an explicit species and estimates the chlorine present based on location, altitude, and solar intensity. Chlorine concentrations are exactly zero during daytime at all locations and altitudes. Nighttime surface-level chlorine concentrations are estimated to be 125 ppt over ocean and coastal areas and 5 ppt over inland areas. Chlorine concentrations are reduced linearly from the surface to zero at a height of 2000 m over ocean and coastal areas or at a height of 1000 m over inland areas.

[16] REMSAD uses the dynamic method described in *Syrakov* [2001] to calculate and track the amount of re-emission of deposited mercury that takes place. This method estimates the rate at which deposited mercury becomes fixed (and unavailable for re-emission) and the rate at which mercury is re-emitted. For land surfaces at a temperature of 25°C, the time to fix half of the deposited mercury is about 1.5 years, while the time to re-emit half of the deposited mercury is about 6 days. These fixation and re-emission rates increase with temperature and are zero below freezing. For ocean surfaces, the half-life for fixation is constant at about 40 years, while the half-life for re-emission is constant at about 6 days.

3.3. TEAM Model

[17] TEAM is a 3-D Eulerian model that simulates the transport, chemical and physical transformations, and removal of Hg species. The original formulation of TEAM was based on a polar stereographic projection [*Pai et al.*, 1997]; this formulation was modified for this study and a Lambert conformal projection was used to allow full compatibility with the meteorological, emission and other inputs used by the other regional-scale models.

[18] Transport processes include transport by the 3-D mean wind flow and dispersion by atmospheric turbulence. Advection is simulated using a semi-Lagrangian numerical scheme. Atmospheric vertical diffusion is simulated with a K-diffusion algorithm. Horizontal diffusion is not treated as it is generally dominated by numerical diffusion in grid-based models.

[19] The chemical transformations of Hg include the gas-phase oxidation of Hg^0 to Hg^{2+} (RGM) by O_3, OH, H_2O_2, and HCl, the aqueous-phase oxidation of Hg^0 to Hg^{2+} by O_3 and OH, the aqueous-phase reduction of Hg^{2+} to Hg^0 by $SO_3^=$ and HO_2, various aqueous-phase equilibria of Hg^{2+} species and the reversible aqueous-phase adsorption of Hg^{2+} to particulate matter (PM). The kinetic parameters, thermodynamic equilibrium parameters and reaction products are provided in *Seigneur et al.* [2006]. Concentrations of the chemical species reacting with Hg species are not simulated in TEAM but instead are input, unlike CMAQ and REMSAD. The chemical species reacting with Hg are obtained from an earlier GEOS-Chem simulation for O_3, SO_2, OH, HO_2 and H_2O_2 and assumed based on available data for HCl, Cl_2 and PM, as described by *Seigneur et al.* [2001]; SO_2 concentrations were refined using CASTNET measurements. The concentrations of HCl and PM are spatially and temporally constant. The concentrations of O_3, SO_2, OH, HO_2 and H_2O_2 are spatially and temporally varying. The concentrations of OH and HO_2 are reduced in the presence of clouds by factors of two and five, respectively, to account for aqueous-phase and heterogeneous reactions of those species in the presence of water droplets.

[20] The calculation of dry deposition is performed using a resistance-transfer approach that is species-specific and depends on land use and meteorology. Dry deposition of Hg^0 is explicitly taken into account. Deposition fluxes are typically reported, as in this study, for Hg^{2+} and PHg because most Hg^0 that is dry deposited is assumed to be re-emitted. In the current model formulation, it is assumed that half of the total deposited Hg (i.e., $Hg^0 + Hg^{2+}$ + PHg) is emitted back to the atmosphere [*Seigneur et al.*, 2004]. Wet deposition includes both removal of Hg present in droplets of precipitating clouds (rainout) and below-cloud scavenging (washout). Rainout is calculated based on the aqueous-phase Hg concentrations calculated by the chemical kinetic mechanism; washout is calculated using scavenging coefficients for Hg^{2+} and PHg.

[21] The horizontal grid resolution is the same as that in CMAQ and REMSAD. The vertical resolution is also similar in this application with 14 layers between the surface and ~14 km altitude with a finer resolution near the surface. However, unlike CMAQ and REMSAD, the layers in TEAM are defined in terms of their height above ground level (agl). These heights were set equal to the domain-wide average height of each CMAQ layer (i.e., 36, 71, 144, 289, 437, 663, 1052, 1541, 2056, 2887, 3906, 5691, 8849 and 14183 m agl).

4. Model Input Data

4.1. Initial and Boundary Conditions for the Regional-Scale Models

[22] All simulation models must be initialized in some way at the starting time of their simulations, and all regional-scale models must specify the conditions at the boundaries of their limited-area domains during their entire simulation period. It is widely recognized that initial conditions are most important early in a simulation and their importance decreases as the simulation progresses, while boundary values can have an important bearing on the entire simulation. Atmospheric Hg remains very under-sampled on the global scale. Even during those limited occasions where atmospheric Hg sampling programs have been conducted, measurements are usually confined to very near the surface. Thus the definition of initial conditions in all three spatial dimensions and lateral boundary conditions at the surface and aloft is often based on previous simulations conducted over a larger spatial domain.

[23] The original plan for the NAMMIS was to employ one or more global-scale models to define a single ''best guess'' initial-condition/boundary-condition (IC/BC) data set for the base-case regional-scale modeling and to arbitrarily perturb that IC/BC definition for test-case analysis of model sensitivity. Eventually, three global-scale models contributed simulation results to the study. On the basis of rather large differences seen in their simulated air concentrations of Hg^0, RGM and PHg at the regional domain boundaries, the study team decided there was no need for any arbitrary perturbation of a ''best guess'' data set. All of the global-scale models employed are based on reasonable scientific definitions and assumptions as described below. Since there are no actual measurements of Hg^0, RGM and PHg air concentrations throughout the depth of the atmosphere on which to base a ''best guess'', each of the global-

scale model simulations was deemed to be a ''reasonable guess'' and was used to define an IC/BC data set for use by the regional-scale models.

[24] All three global models used the same anthropogenic Hg emission inventory based on the 1995 global inventory by *Pacyna et al.* [2003] with updates to the year 2000 for Europe as employed in the MSC-East model intercomparison study [*Ryaboshapko et al.*, 2007a]. The global emission data were further updated to the year 2001 for the U.S. and Canada based on information developed for the CAMR modeling [*US EPA*, 2005b]. Mexican emissions were updated based on information from a study sponsored by the Commission for Environmental Cooperation [*CEC*, 2004]. Emissions for all other continents were scaled to 2000 estimates from *Pacyna et al.* [2006].

[25] For other pollutant species besides Hg^0, RGM and PHg, boundary air concentrations were also defined on a monthly-averaged basis for use in CMAQ and REMSAD. These two models used non-Hg air concentrations obtained from a GEOS-Chem model simulation of ozone-NOx-hydrocarbon-aerosol chemistry [*Park et al.*, 2004]. By using the same non-Hg air concentrations for the regional-scale simulation tests for CMAQ and REMSAD, a clearer indication of the effect of uncertainty regarding Hg air concentrations could be gained. TEAM does not require boundary air concentrations of non-Hg species because the concentrations of the chemical species reacting with Hg are not simulated but instead are specified in the model (see earlier discussion).

4.1.1. Chemical Transport Model for Mercury (CTM-Hg)

[26] The global chemical transport model for Hg (CTM-Hg) has been described in detail elsewhere [*Shia et al.*, 1999; *Seigneur et al.*, 2001]. The model provides a horizontal resolution of 8° latitude and 10° longitude and a vertical resolution of nine layers ranging from the Earth's surface to the lower stratosphere. Seven layers represent the troposphere (between the surface and ~12 km altitude) and two layers the stratosphere (between ~12 km and 30 km altitude). Transport processes are driven by a generic simulated meteorological gridded data set, which includes the wind fields and convection statistics calculated every 4 hours (for an entire year) by the Goddard Institute for Space Studies (GISS) general circulation model [*Hansen et al.*, 1983].

[27] The Hg transformation processes include the same gas-phase transformations, gas/droplet equilibria, ionic equilibria, solution/particle adsorption equilibrium, and aqueous-phase transformations as those simulated in TEAM. The chemical species reacting with Hg are input to the model as described by *Seigneur et al.* [2001]. Dry deposition of Hg is simulated with deposition velocities that are 0.5, 0.1 and 0.01 cm/s for RGM, PHg and Hg^0, respectively, over land and 0.5, 0.01 and 0 cm/s for RGM, PHg and Hg^0, respectively, over water. Wet deposition is simulated using the calculated Hg concentrations in cloud droplets for rainout and scavenging efficiencies for washout (100, 50 and 0% for RGM, PHg and Hg^0, respectively). The CTM-Hg is run repeatedly for several years until steady state is achieved. The global CTM-Hg provides boundary conditions for the continental simulations as follows. Initial and boundary conditions of Hg^0, RGM and PHg were obtained from the global (8° × 10° resolution) grid cells between 16°N and 64°N latitude and 150°W and 40°W longitude. These grid cells in the bottom seven vertical levels of the global grid were mapped to the fourteen layers of the continental modeling grid. Monthly average concentrations were calculated for use as initial and boundary conditions for the continental model simulations.

4.1.2. GEOS-Chem Model

[28] The GEOS-Chem mercury simulation is described in detail by *Selin et al.* [2007]. The simulation for NAMMIS was conducted at a horizontal resolution of 2° × 2.5° using GEOS-Chem version 7.01 (http://www-as.harvard.edu/chemistry/trop/geos/) [*Bey et al.*, 2001]. Three species of atmospheric mercury are simulated: Hg^0, Hg^{2+} and primary PHg. Primary PHg is assumed to be non-volatile and chemically inert. Natural and re-emissions of mercury are included as described by Selin et al., and ocean emissions are specified as a function of latitude. The simulated chemistry includes Hg^0 oxidation to Hg^{2+} by OH ($k = 9 \times 10^{-14}$ cm^3 s^{-1} [*Pal and Ariya*, 2004; *Sommar et al.*, 2001]) and ozone ($k = 3 \times 10^{-20}$ cm^3 s^{-1} [*Hall*, 1995]). It also includes aqueous-phase photochemical reduction of Hg^{2+} to Hg^0 as an in-cloud photochemical process applied to dissolved Hg^{2+} and scaled to match constraints on total gaseous mercury (TGM) lifetime and seasonal variation as described by Selin et al. Wet deposition of mercury in GEOS-Chem is applied to Hg^{2+} and PHg, and includes rainout and washout from large-scale and convective precipitation, and scavenging in convective updrafts [*Liu et al.*, 2001]. The simulation assumes that Hg^{2+} is scavenged quantitatively by liquid precipitation, and that PHg is scavenged with the same efficiency as a water-soluble aerosol [*Liu et al.*, 2001]. Dry deposition of Hg^{2+} and PHg is simulated with a standard resistance-in-series scheme based on local surface type and turbulence [*Wang et al.*, 1998; *Wesely*, 1989] assuming zero surface resistance for Hg^{2+}. Output for NAMMIS was provided at three-hour averages for the year 2001 at horizontal resolution of 2° × 2.5°. These three-hour data were subsequently used by the U.S. EPA to compute the monthly-averaged boundary values used by the regional-scale models.

4.1.3. Global/Regional Atmospheric Heavy Metals (GRAHM) Model

[29] The Global/Regional Atmospheric Heavy Metals (GRAHM) model is an Eulerian, multi-scale meteorological and mercury simulation model which was developed by including atmospheric mercury dynamical, physical and chemical processes on-line into the Canadian operational weather forecasting and data assimilation model, namely the Global Environmental Multiscale (GEM) model. The main features of GRAHM are described by *Dastoor and Larocque* [2004] and *Ariya et al.* [2004]. Transport, transformation and surface exchange of three mercury species, namely, gaseous Hg^0, gaseous Hg^{2+} (the same as RGM) and PHg are simulated in the model. Natural and re-emissions of mercury as Hg^0 over the oceans and land are based on the global mercury budget study by *Mason and Sheu* [2002]. These emissions are spatially distributed according to the primary production activity over the oceans and according to the mercury content in soils, distribution of previously deposited mercury and the surface temperature over land. Diurnal and seasonal variations are introduced as a function

of the surface solar irradiance. Following the discussion in *Calvert and Lindberg* [2005] and the observational constraints of mercury measurements on a global scale, GRAHM was adapted to use the slow oxidation of gaseous Hg^0 by O_3 reported in *Hall* [1995] as the only oxidation of Hg^0 in the gas phase. Monthly averaged and diurnally varying concentrations of O_3 are adapted from a detailed tropospheric chemistry model MOZART [*Horowitz et al.*, 2003]. Half of the oxidation product is considered as Hg^{2+} and the other half as PHg. Oxidation of Hg^0 by O_3, OH and reactive chlorine and reduction of Hg^{2+} by S(IV) and via photolysis of $Hg(OH)_2$ are part of the aqueous phase redox chemistry in the model [*Lin and Pehkonen*, 1999]. Sorption of aqueous mercury species to elemental carbon aerosols is also included in the model. Hg^0 is dry deposited only over forest regions because of its low solubility and it is modeled using a seasonally dependent constant dry deposition velocity in the range of 0.001–0.03 cm s^{-1} [*Lindberg et al.*, 1991]. Dry deposition of Hg^{2+} is parameterized utilizing the multiple resistance analogy approach as described in *Zhang et al.* [2003]. Dry deposition velocity for PHg is parameterized as a function of particle size and density [*Zhang et al.*, 2001]. Both gaseous and particle dry deposition velocities are functions of micro-meteorological conditions, land-use types, surface wetness, snow/ice and surface roughness characteristics. GRAHM, being an on-line model, has the advantage of using detailed cloud micro-physical parameters which are simulated at each time step by the model cloud parameterization schemes which are used for the formation of wet deposition in the model. Mercury removal through the conversion of hydrometeors to precipitation as well as through below cloud scavenging are included in the model. Model simulation for NAMMIS was conducted at $5^0 \times 5^0$ horizontal resolution, 28 levels in the vertical with a model top at 10 mb. The model simulation results for the year 2001 were generated at 6 hourly frequency. These 6-hour data were subsequently used by the U.S. EPA to compute the monthly-average boundary values used by the regional-scale models.

4.2. Lateral Boundary Air Concentration Profiles

[30] The global-scale models described above were each used to define monthly average air concentrations of Hg^0, RGM and PHg across all four of the lateral boundaries of the regional modeling domain. For other pollutants that react with Hg in any or all of the regional-scale models (e.g., O_3 and OH), a single IC/BC definition was developed for CMAQ and REMSAD for each month from the GEOS-Chem model simulation.

[31] The IC/BC data sets provided two-dimensional patterns of Hg^0, RGM and PHg air concentrations across each lateral boundary (north, east, south and west) for each month of 2001. For a simplified illustration of the differences between the three global-scale models, horizontally-averaged vertical profiles for each lateral boundary have been developed. Average air concentration profiles for Hg^0, RGM and PHg for February and July 2001 are shown in Figures 1, 2, and 3, respectively. The GRAHM model simulated slightly lower Hg^0 air concentrations than the other two global models, especially at higher altitudes (Figure 1). The GEOS-Chem model simulated considerably higher concentrations of RGM in the upper layers than the other models, except along the southern boundary (Figure 2). Also, the CTM-Hg tended to show higher RGM concentrations than the other global models in the middle troposphere during July, but lower concentrations at higher altitudes. The GRAHM model simulated much higher PHg concentrations, especially in the upper half of the vertical domain, while the other two global models show very little PHg at any height (Figure 3). The GRAHM model simulated strong oxidation of Hg^0 by stratospheric ozone to produce PHg in addition to RGM at high altitudes while the other two global models produced negligible PHg. Indeed, GEOS-Chem characterizes PHg as primary aerosol only and all of its Hg oxidation products are treated as a general Hg^{2+} species. Although there are insufficient Hg data aloft to evaluate the discrepancies among these three global models, it is interesting to note that recent data suggest that Hg near the tropopause (upper troposphere and lower stratosphere) is mostly oxidized PHg [*Murphy et al.*, 2006].

4.3. Pollutant Emissions Data

[32] The anthropogenic Hg emissions for all three regional-scale models were prepared from the CAMR inventory [*US EPA*, 2005b]. An inventory of Hg emissions from oceans, land surfaces and volcanic activity from *Seigneur et al.* [2004] was also used by all three regional-scale models. Emissions files for non-Hg species for the CMAQ and REMSAD simulations were prepared using the emissions inventory used in modeling in support of the Clean Air Interstate Rule (CAIR) [*US EPA*, 2005c]. As described above, the TEAM model utilized GEOS-Chem results to define air concentrations for non-Hg species and therefore did not require specifying an emissions inventory for non-Hg emissions.

[33] Approximately 115 tons of Hg in all forms were emitted from anthropogenic sources in the U.S. and Canada in 2001 based on this inventory. Emissions of Hg from Mexico were not accounted for in the CAMR inventory because of a lack of sufficient information on individual source location and exhaust stack parameters. Although Hg emissions from Mexico have little influence on Hg deposition in the northeastern United States [*Seigneur et al.*, 2003], not including Mexican Hg emissions may lead to some underestimation of Hg deposition in other areas of the United States.

4.4. Meteorological Data

[34] Meteorological conditions influence the formation, transport, and deposition of air pollutants. The regional-scale models applied in this study all require a specific suite of meteorological input data in order to simulate these physical and chemical processes. For the NAMMIS, we used the same meteorological input data source as previously used by the U.S. EPA in its development of the CAMR. Meteorological data for the entire 2001 test period were obtained from a simulation of the Pennsylvania State University/National Center for Atmospheric Research Mesoscale Model – Generation 5 [*Grell et al.*, 1994]. This model, commonly referred to as MM5, is a limited-area, non-hydrostatic model employing a terrain-following σ_P vertical coordinate system. The MM5 solves for the full set of physical and thermodynamic equations which govern atmospheric motions. Version 3.6.1 of the MM5 model code was used. The MM5 horizontal domain consisted of an

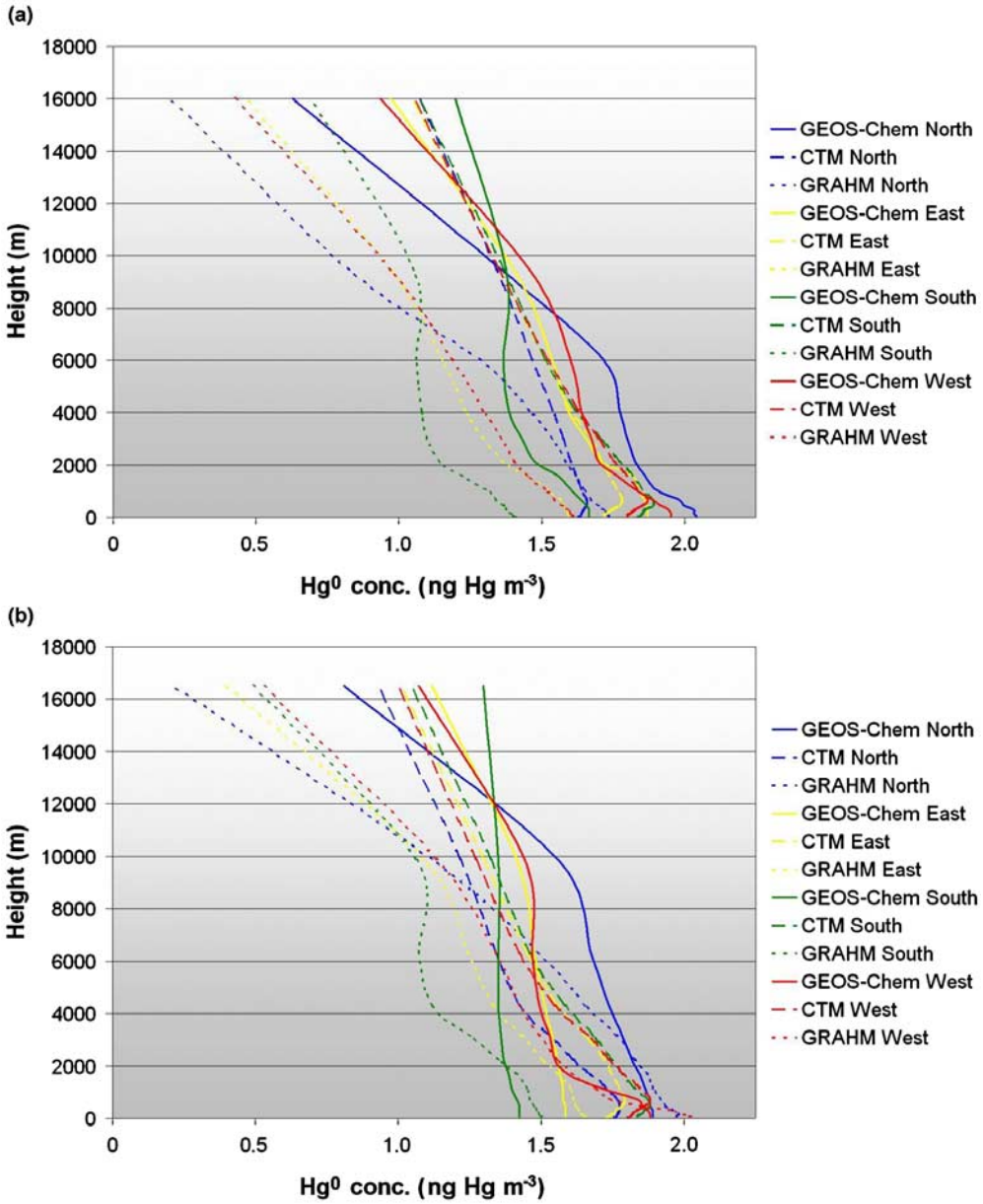

Figure 1. Vertical profiles of the average lateral boundary air concentrations of Hg^0 from the CTM-Hg, GEOS-Chem, and GRAHM global-scale models for (a) February and (b) July of 2001.

array of 165 by 129 grid cells, selected to completely cover the regional-scale modeling domain with an adequate marginal buffer to avoid boundary effects in the meteorological data sent to the air quality models. The MM5 modeling used 34 vertical layers with a surface-contact layer depth of approximately 38 meters and a model top boundary at the 10 kPa (100 millibar) pressure level.

[35] A very important aspect of the meteorological guidance provided to the regional-scale atmospheric mercury models is the placement and intensity of precipitation. Comparisons of MM5-simulated precipitation amounts to observations at the MDN locations have found some overestimation of precipitation depth and low statistical correlation during the summer of 2001 [*Bullock and Brehme*, 2002]. The effects of these inaccuracies in precipitation on weekly, seasonal and annual Hg wet deposition model statistics are still being investigated and the results will be reported in a future publication.

5. Comparison of Simulated Air Concentrations

[36] Annual average air concentrations of Hg^0, RGM and PHg as simulated by the three regional-scale models for the 2001 study period were computed for layer 1 (surface-level) and layer 10 (approx. 3000 m altitude). Because of the differing vertical coordinates in TEAM versus the other models, its layer-10 boundaries may differ by up to 200 meters from those of the other models. These concentrations were calculated in units of Hg mass per "standard" volume of air at 273 K and 1 atm.

[37] Figure 4 displays a 3-by-3 array of annual-average surface-layer Hg^0 air concentration patterns simulated by all

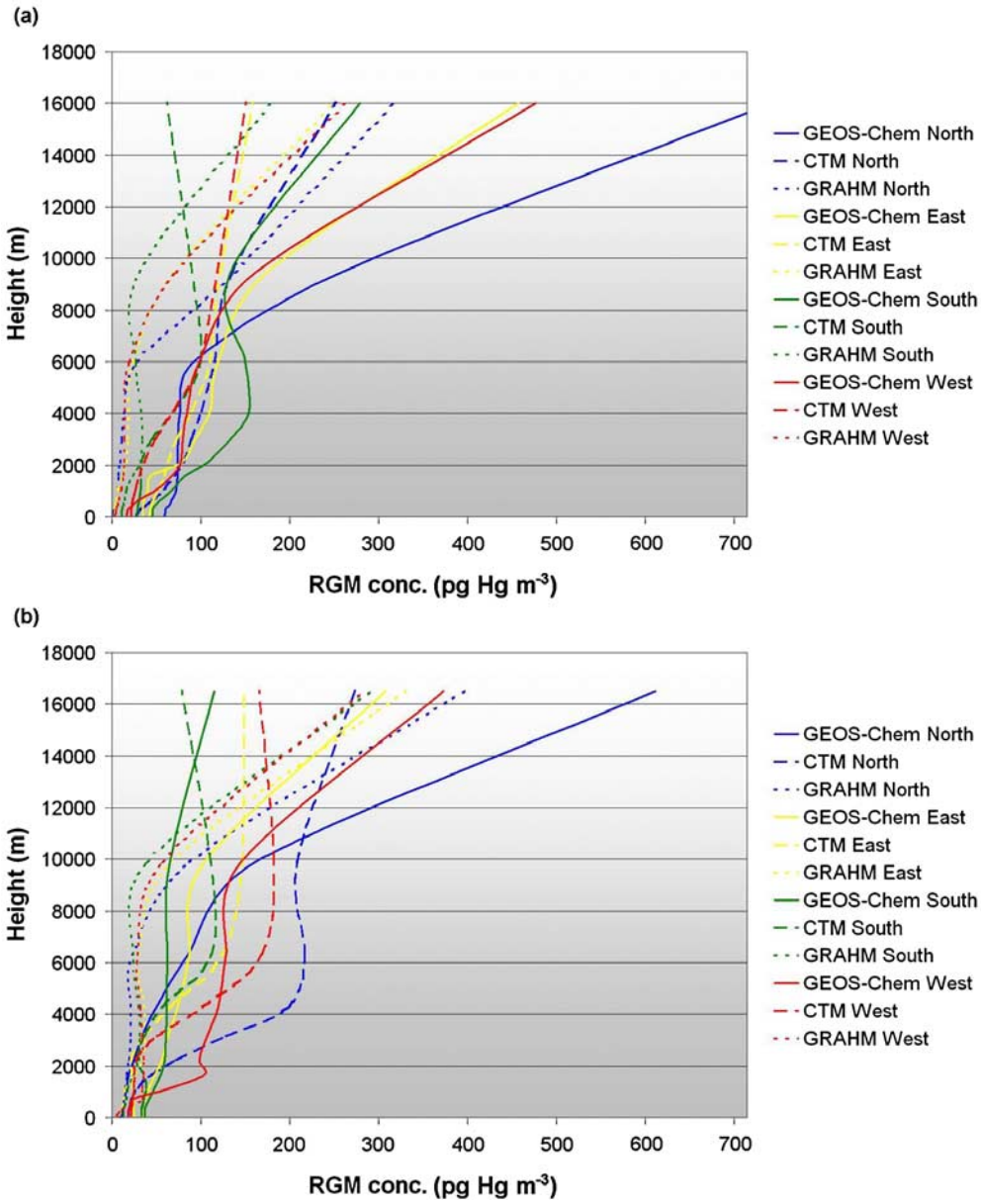

Figure 2. Vertical profiles of the average lateral boundary air concentrations of RGM from the CTM-Hg, GEOS-Chem, and GRAHM global-scale models for (a) February and (b) July of 2001.

three regional-scale models using all three IC/BC data sets. The same Hg^0 air concentration information for layer 10 in each model (approx. 3000 m altitude) is presented in Figure 5. All three regional-scale models produce a general south-to-north gradient in Hg^0 air concentrations at both levels when the GEOS-Chem and GRAHM boundary values are used. As shown in Figure 1, these two global models simulated higher Hg^0 concentrations along the northern boundary than for the southern boundary below altitudes of about 10 km, with much the opposite relationship well above 10 km. While there is considerable variation among the regional-scale models in the Hg^0 concentration patterns they produce due to other factors, the influence of boundary values for this species is obvious.

[38] The TEAM model shows obvious depletion of surface-level Hg^0 in the Tennessee and Ohio River Valley areas and in the Northeast U.S. where atmospheric chemistry is more conducive to oxidation. The CMAQ and REMSAD models simulate their lowest surface-level Hg^0 concentrations over the western U.S. and Mexico while the TEAM model simulates its lowest values at varying locations further east depending on the IC/BC data set used. Some depression of surface-level concentrations in high terrain is expected because of the declining concentrations with height in the IC/BC data sets (Figure 1). However, this characteristic is very strong in the REMSAD results and it remains strong even as high as layer 10 as seen in Figure 5. These exceedingly low Hg^0 concentrations over high terrain

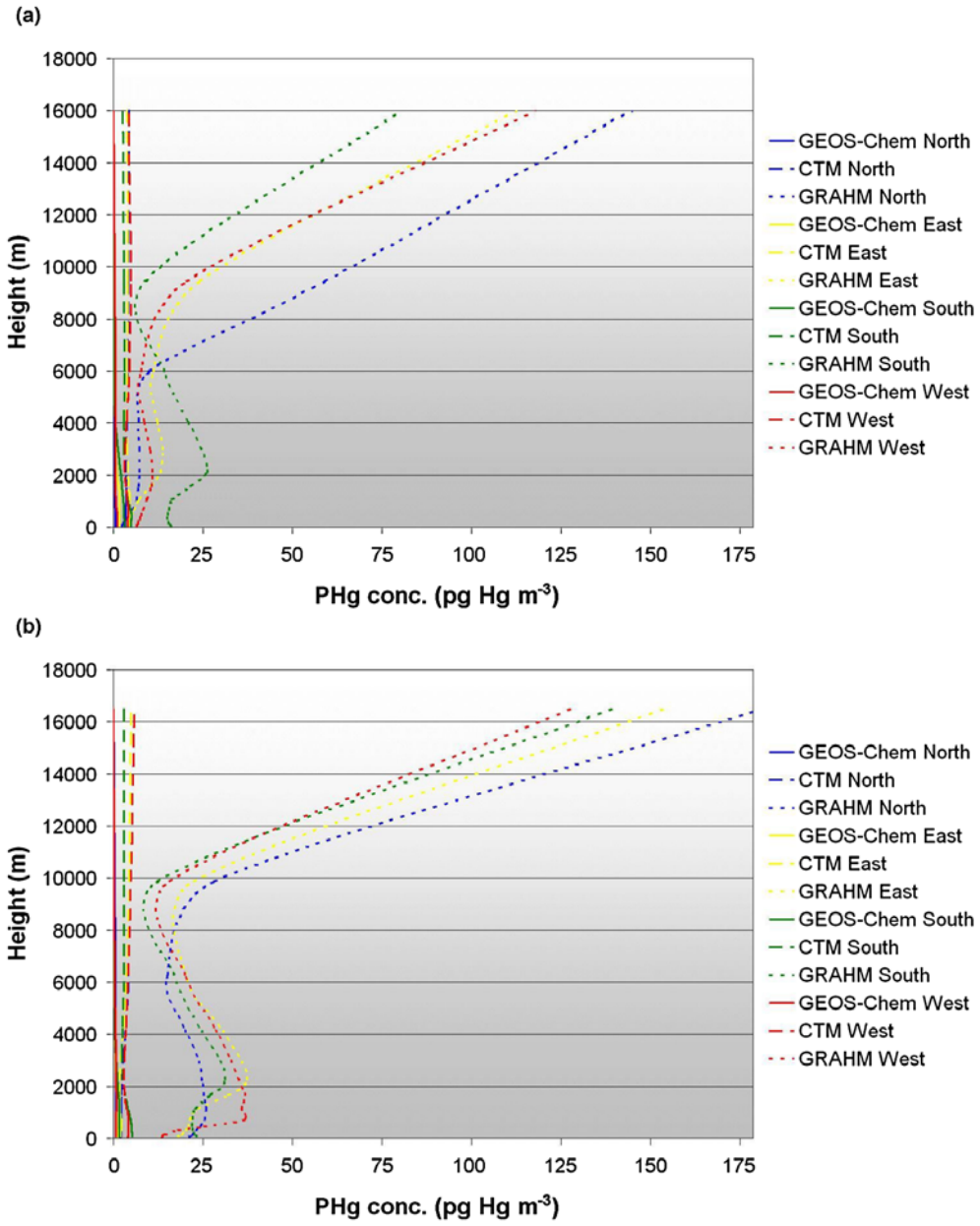

Figure 3. Vertical profiles of the average lateral boundary air concentrations of PHg from the CTM-Hg, GEOS-Chem, and GRAHM global-scale models for (a) February and (b) July of 2001.

were investigated by ICFI and found to be an artifact of the REMSAD model's treatment of wind flow over high terrain.

[39] Figures 6 and 7 present annual-average RGM air concentrations for model layers 1 and 10, respectively, as simulated by each of the three regional-scale models using each of the three IC/BC test data sets. Generally, the highest RGM concentrations are simulated by the REMSAD model and the lowest are simulated by the CMAQ model. The average surface-layer concentrations of RGM from the REMSAD simulations exceed 50 pg m^{-3} over large areas, especially for the GEOS-Chem IC/BC case. The TEAM model also shows annual average surface-level RGM concentrations over 50 pg m^{-3}, but for somewhat smaller areas. The CMAQ model shows much lower RGM concentrations in the surface layer than the other two models, with values over 50 pg m^{-3} largely confined to the most industrialized locations. For layer 10, there is less difference between the regional-scale models in their simulated RGM concentrations. REMSAD remains the model with the highest RGM concentrations for most locations, but the TEAM model shows the lowest RGM concentrations at this level. Note that the scale of RGM concentrations is doubled in Figure 7 (layer 10) versus Figure 6 (layer 1). All three regional-scale models simulated much higher concentrations of RGM well above the surface, much like all three global-scale models did in the development of the IC/BC data sets.

[40] Figures 8 and 9 display annual-average PHg air concentrations for layers 1 and 10, respectively. The

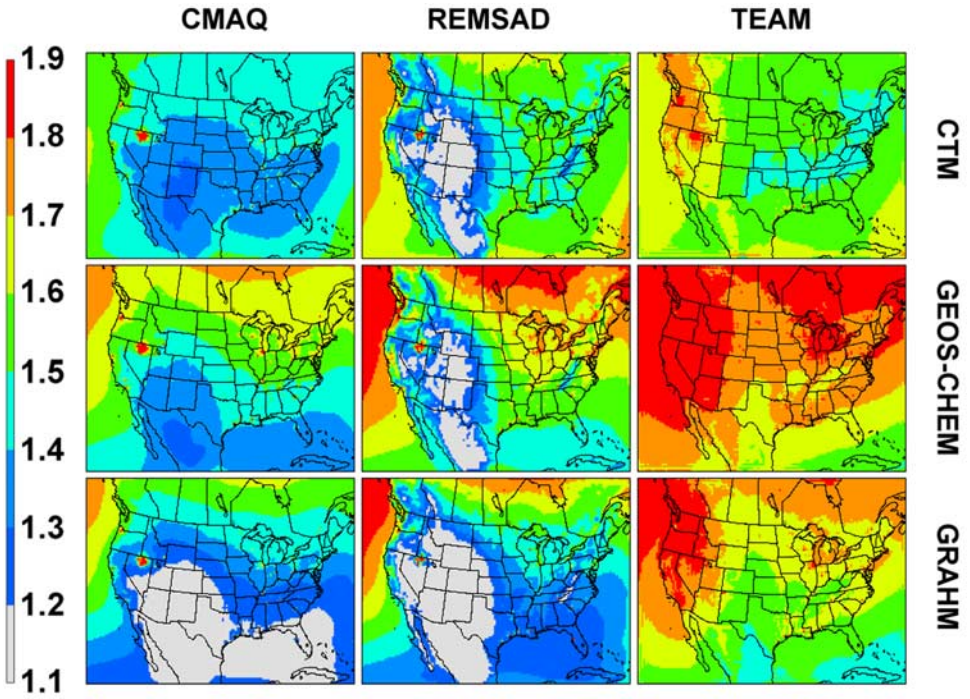

Figure 4. Annual average surface-level air concentration of Hg^0 (nanograms per cubic meter of standard air) as simulated by the CMAQ, REMSAD, and TEAM models using the IC/BC inputs from the CTM-Hg, GEOS-Chem, and GRAHM global models.

REMSAD and TEAM models simulate relatively little PHg at either level, except for layer 10 in the GRAHM IC/BC case where high PHg concentration are found which lead to significant concentrations across the entire horizontal domain. The GRAHM IC/BC case also specified relatively high PHg concentrations for layer 1, but the effect in the interior of the regional modeling domain appears to be moderated by simulated deposition from this surface-con-

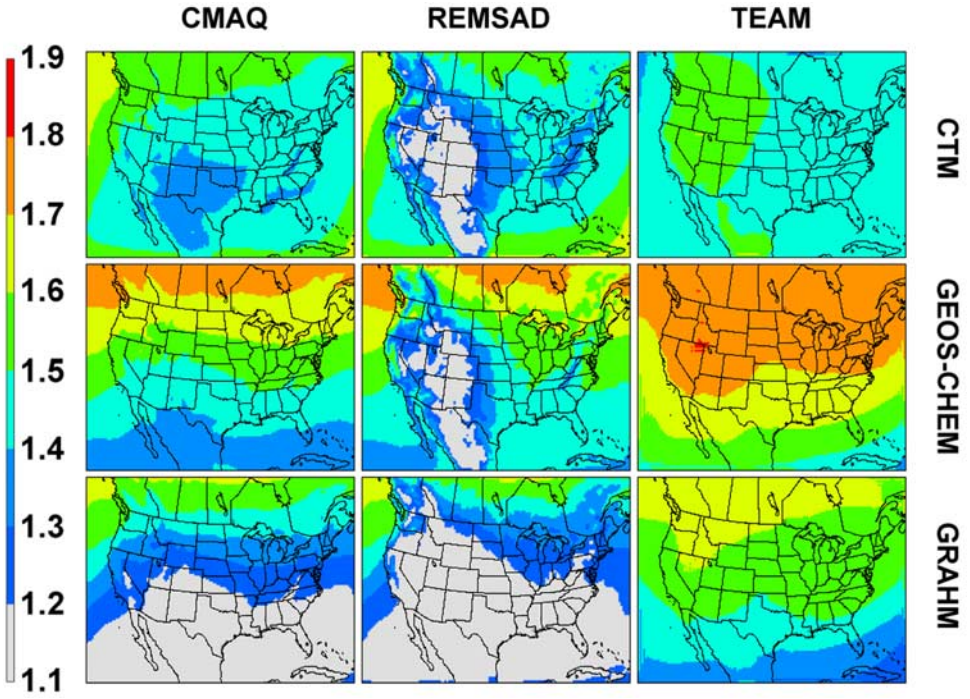

Figure 5. Annual average layer-10 (approximately 3 km altitude) air concentration of Hg^0 (nanograms per cubic meter of standard air) as simulated by the CMAQ, REMSAD, and TEAM models using the IC/BC inputs from the CTM-Hg, GEOS-Chem, and GRAHM global models.

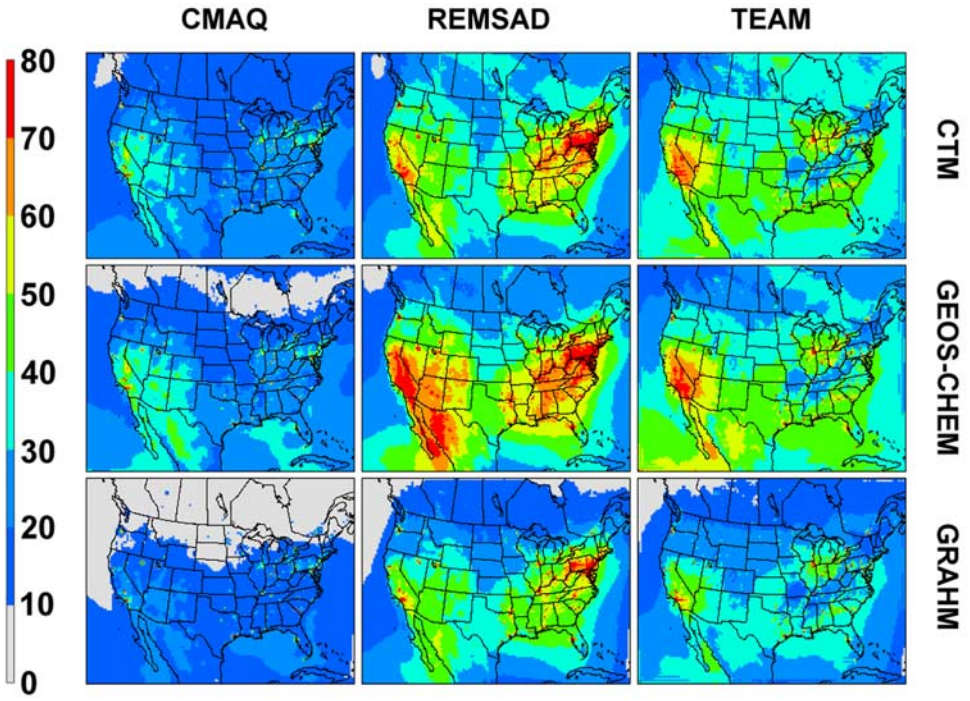

Figure 6. Annual average surface-level air concentration of RGM (picograms per cubic meter of standard air) as simulated by the CMAQ, REMSAD, and TEAM models using the IC/BC inputs from the CTM-Hg, GEOS-Chem, and GRAHM global models.

tact layer. The CMAQ model simulates annual average surface-level PHg concentrations of over 20 pg m^{-3} across most of the U.S. and northern Mexico for all three test cases, while at layer 10 it simulates about half as much PHg over that same area except for the GRAHM IC/BC case where boundary value effects are once again evident. Note that the scale of PHg concentrations is halved in Figure 9 (layer 10) versus Figure 8 (layer 1). REMSAD and TEAM

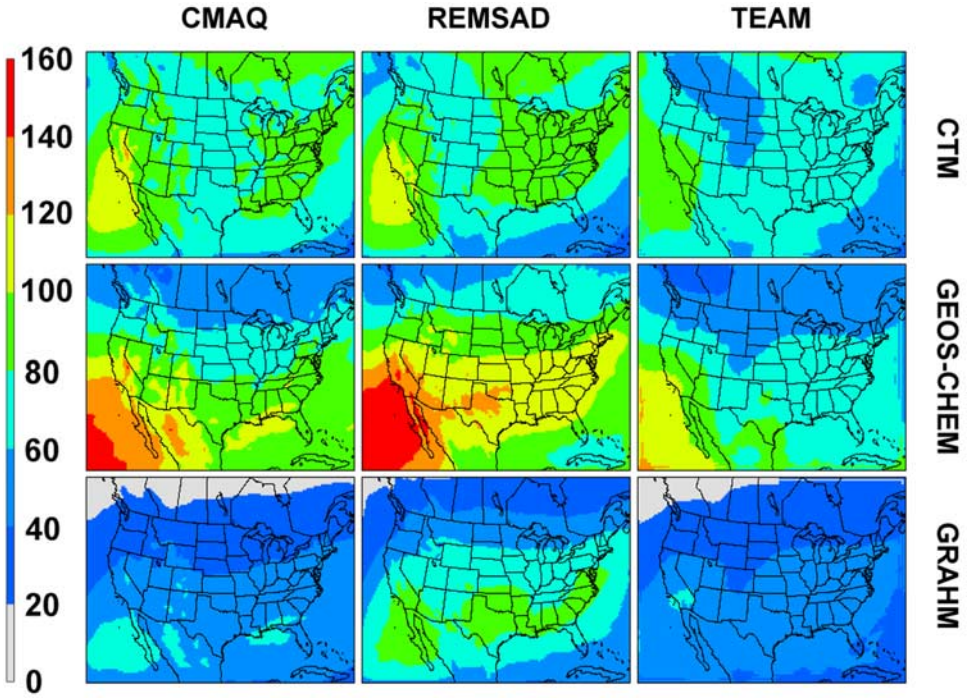

Figure 7. Annual average layer-10 (approximately 3 km altitude) air concentration of RGM (picograms per cubic meter of standard air) as simulated by the CMAQ, REMSAD, and TEAM models using the IC/BC inputs from the CTM-Hg, GEOS-Chem, and GRAHM global models.

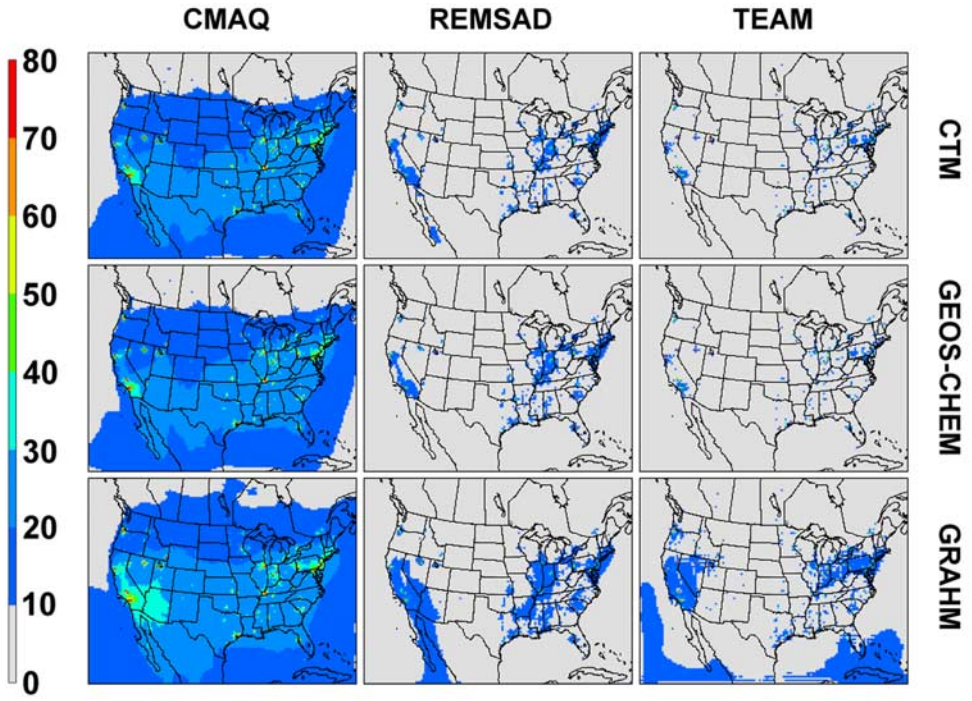

Figure 8. Annual average surface-level air concentration of PHg (picograms per cubic meter of standard air) as simulated by the CMAQ, REMSAD, and TEAM models using the IC/BC inputs from the CTM-Hg, GEOS-Chem, and GRAHM global models.

simulate PHg concentrations that are significantly lower than RGM concentrations in virtually all situations. CMAQ also simulates less PHg than RGM in layer 10, but to a smaller degree. At the surface, CMAQ simulates slightly less PHg than RGM when the CTM-Hg and GEOS-Chem IC/BC data are used and slightly more PHg than RGM when the GRAHM IC/BC data are used.

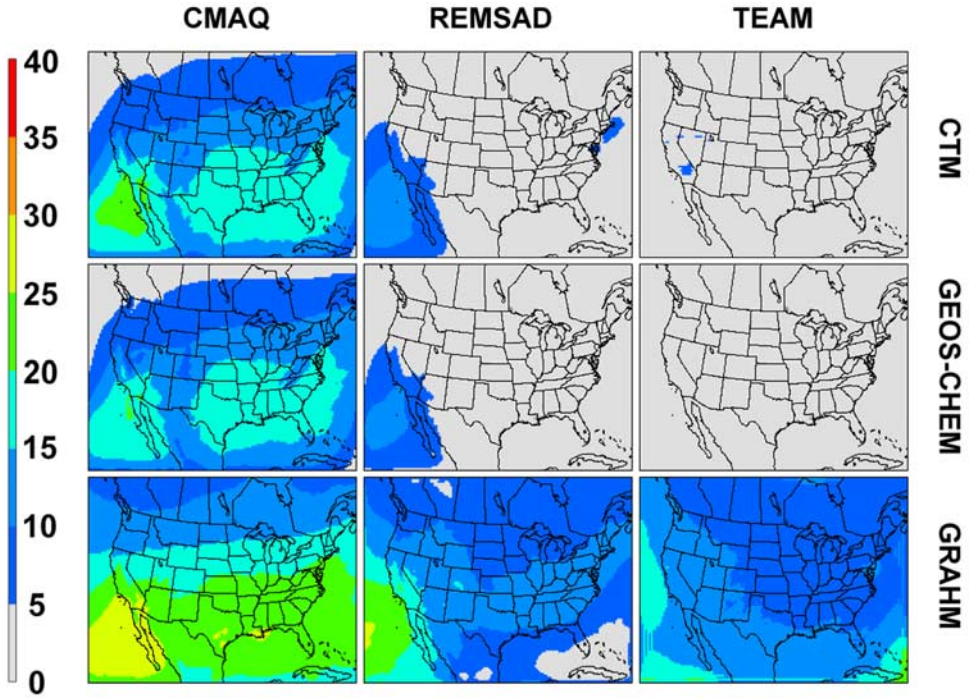

Figure 9. Annual average layer-10 (approximately 3 km altitude) air concentration of PHg (picograms per cubic meter of standard air) as simulated by the CMAQ, REMSAD, and TEAM models using the IC/BC inputs from the CTM-Hg, GEOS-Chem, and GRAHM global models.

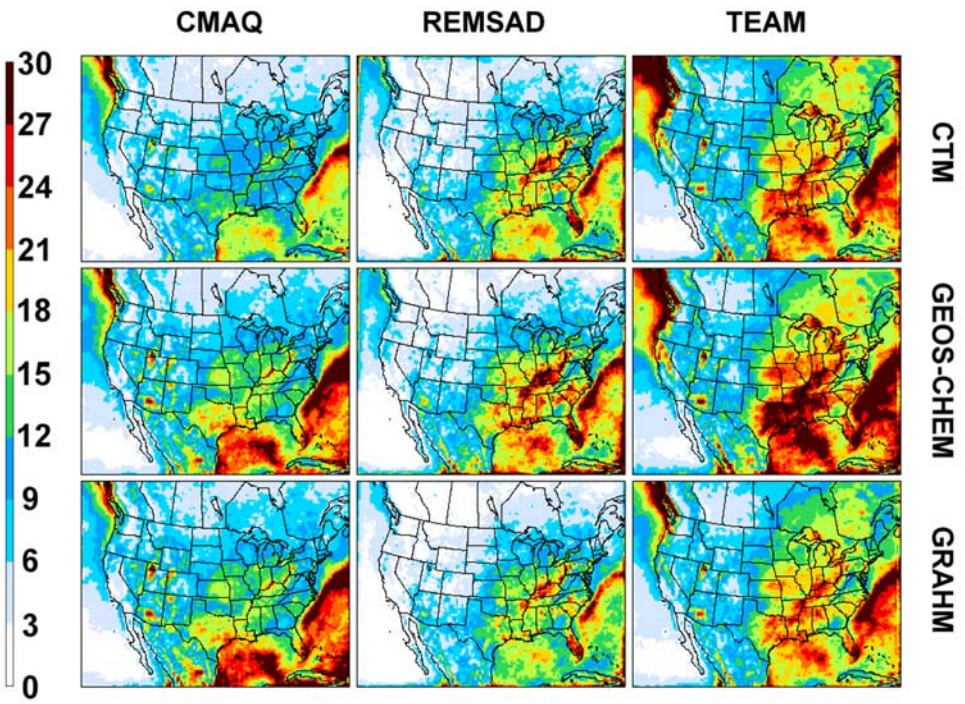

Figure 10. Annual wet deposition flux of all forms of mercury (micrograms per square meter) as simulated by the CMAQ, REMSAD, and TEAM models using the IC/BC inputs from the CTM-Hg, GEOS-Chem, and GRAHM global models.

6. Comparison of Simulated Deposition

[41] Patterns of annual wet deposition flux for total Hg (Hg^0, RGM and PHg combined) as simulated by each of the three regional-scale models from each of the three IC/BC test cases are shown in Figure 10 using the same 3-by-3 array configuration employed in the illustration of air concentration patterns. Wet deposition flux is obviously influenced to a great degree by the amount of precipitation. Figure 11 shows the total precipitation depth (liquid equivalent) as input to the regional-scale models from the MM5 simulation. Since all three regional-scale models used the same precipitation input data, the areas of high and low wet deposition are quite similar between models and between IC/BC cases. However, the overall magnitude of wet deposition in these patterns does vary considerably.

[42] Most of the simulations show very high wet deposition totals near Vancouver Island, over the Gulf Stream and over the Gulf of Mexico. The wet climate of Vancouver Island is well known. Precipitation is not routinely measured over the Gulf Stream or in the Gulf of Mexico, but it is reasonable to expect heavy precipitation over these warm waters and the MM5 model simulation did indeed produce large annual precipitation totals over all of these areas. Unfortunately, there were no measurements of Hg wet deposition flux for 2001 in any of these areas.

[43] In general, the CMAQ model simulated the least amounts of Hg wet deposition over land areas of the U.S. and Canada as compared to the other regional-scale models. The REMSAD model simulated slightly more Hg wet deposition over land areas than CMAQ, while the TEAM model simulated the most over land by a large margin. The REMSAD simulated the least Hg wet deposition over the oceanic areas where precipitation was heaviest and where CMAQ and TEAM simulated much more Hg wet deposition. Each of these models generally showed the most wet deposition of Hg when the GEOS-Chem IC/BC data set was used and the least with the CTM-Hg IC/BC data set, but there was some model-to-model variability in this regard.

[44] Figure 12 presents the 3-by-3 array of Hg dry deposition patterns simulated by the regional-scale models. There was much more model-to-model variation in the patterns of dry deposition of Hg than was the case for wet deposition, both in terms of the location of the minima and maxima and in terms of the general magnitude. The REMSAD model simulated much less dry deposition of Hg than the CMAQ and TEAM models. The CMAQ model simulated its strongest dry deposition over the high terrain of California and northern Mexico with a secondary maximum over the northeast U.S. The TEAM model simulated its strongest dry deposition of Hg over interior sections of the northeast U.S. and over the Ohio River Valley, with small areas of strong dry deposition also over the high terrain of the western U.S. and northern Mexico. Because dry deposition of Hg is not directly measured by any operational network, it is difficult to assess the realism of any of these simulated patterns. However, dry deposition has been identified as a significant contributor to the total atmospheric deposition of Hg in many situations [*Lindberg and Stratton*, 1998; *Rea et al.*, 2000; *Poissant et al.*, 2004; *Gustin et al.*, 2006; *Lyman et al.*, 2007]. Development and deployment of Hg dry deposition measurement technology is a critical need for future development and evaluation of atmospheric mercury models.

[45] Table 2 shows an accounting of mercury deposition to the NAMMIS modeling domain as simulated by each of

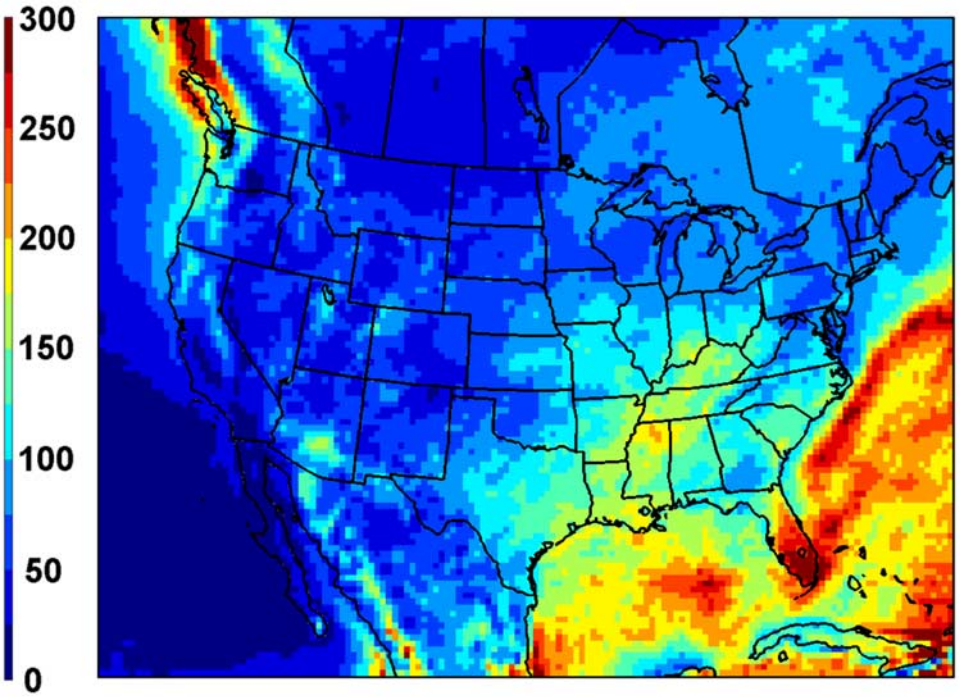

Figure 11. Annual total liquid-equivalent precipitation depth (cm) as simulated by MM5 and used as input to the three regional-scale models.

the three regional models using each of the three IC/BC sets. The deposition indicated is for the entire domain with the exception of the outermost grid cells. TEAM simulated the greatest wet deposition flux of mercury overall while CMAQ simulated the least. In all cases, the vast majority of simulated Hg wet deposition was in the form of RGM. REMSAD simulated very little wet deposition of PHg. None of the models simulated much wet deposition of Hg^0 using any of the IC/BC data sets as expected because of the extremely low solubility of Hg^0 in water. Dry

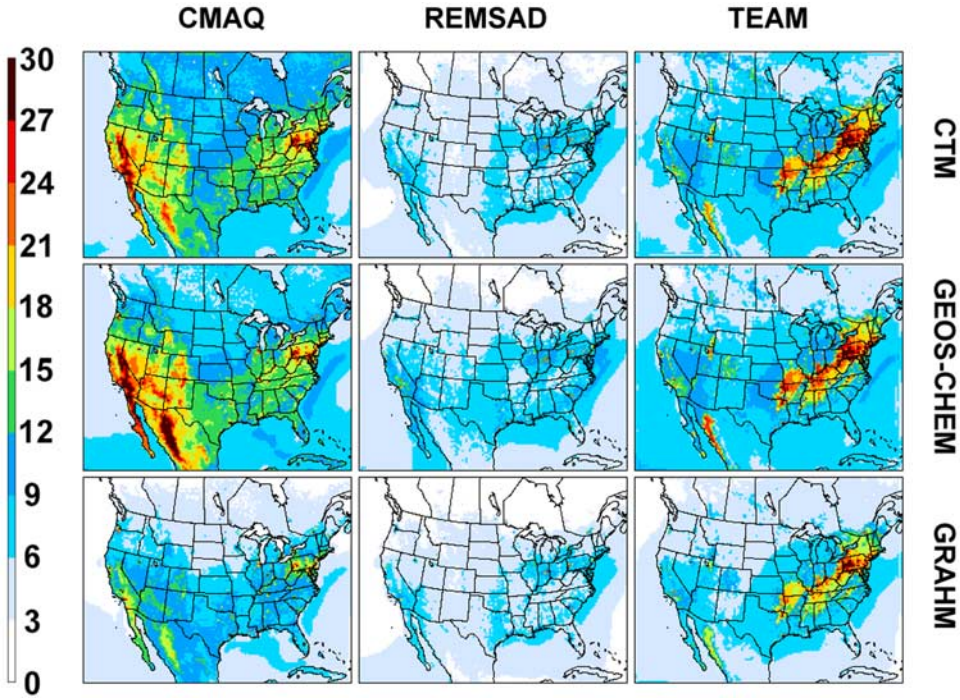

Figure 12. Annual dry deposition flux of all forms of mercury (micrograms per square meter) as simulated by the CMAQ, REMSAD, and TEAM models using the IC/BC inputs from the CTM-Hg, GEOS-Chem, and GRAHM global models.

Table 2. Simulated Mercury Deposition for the NAMMIS Modeling Domain in 2001 (Kilograms)

Model	CMAQ			REMSAD			TEAM		
IC/BC set	CTM-Hg	GEOS-Chem	GRAHM	CTM-Hg	GEOS-Chem	GRAHM	CTM-Hg	GEOS-Chem	GRAHM
				Wet Deposition					
Hg^0	100	103	86	61	63	55	98	110	94
RGM	136,723	193,473	152,382	189,378	211,807	166,313	294,386	329,073	208,022
PHg	47,659	46,525	88,797	504	471	628	15,517	7080	65,489
Total Hg	184,482	240,102	241,265	189,942	212,340	166,995	310,002	336,262	273,605
				Dry Deposition					
RGM	209,089	208,090	125,436	48,926	55,822	43,720	164,129	166,996	120,253
PHg	4715	4628	5582	4518	4508	6115	4386	3061	11,271
Total Hg	213,804	212,718	131,018	53,445	60,330	49,834	16,8516	170,057	131,523
				All Deposition					
Hg^0	100	103	86	61	63	55	98	110	94
RGM	345,812	401,563	277,818	238,304	267,628	210,033	458,516	496,069	328,275
PHg	52,374	51,153	94,379	50,22	4980	6742	19,903	10,141	76,760
Total Hg	398,286	452,819	372,283	243,387	272,670	216,829	478,517	506,319	405,129

deposition of Hg^0 was not treated by CMAQ or REMSAD. TEAM did simulate dry deposition of Hg^0, but it did not report dry deposition fluxes of Hg^0 because most Hg^0 that is dry deposited is assumed to be emitted back to the atmosphere. In all models and for all cases, RGM was the primary species of Hg dry deposited. Minor dry deposition fluxes of PHg were simulated by all models, but these fluxes were very small because all of the models treated PHg as a fine aerosol with a minimal deposition velocity. In terms of the total (wet + dry) deposition flux of all forms of Hg, TEAM simulated the largest flux to the NAMMIS modeling domain, followed closely by CMAQ, with REMSAD simulating the least overall because of its much smaller dry deposition component.

7. Discussion and Summary

[46] RGM is widely accepted as the species of Hg most readily deposited from the atmosphere. CMAQ generally simulated lower RGM concentrations at the surface than did REMSAD and TEAM. One might expect CMAQ to have somewhat lower RGM concentrations than TEAM because CMAQ simulates the gaseous reactions of ozone and OH with Hg^0 making 50% RGM and 50% PHg while TEAM produces 100% RGM from these reactions. However, REMSAD treats these two reactions in the same way as CMAQ, so the observed differences in RGM air concentration cannot be due to differing chemistry alone. Differences in the treatments of dry deposition and/or vertical mixing could also be a factor, as could a number of other internal model mechanisms the investigation of which is beyond the scope of this study.

[47] CMAQ simulated considerably higher air concentrations of PHg both at the surface and aloft than did REMSAD and TEAM. While TEAM produces no PHg in its simulated chemical reaction products, CMAQ and REMSAD both do as mentioned in the previous paragraph. The higher PHg concentrations from CMAQ are likely due to the sorption of dissolved RGM to suspended carbon particles in its cloud chemistry mechanism, which leads to PHg production upon cloud evaporation. Air concentrations are calculated in CMAQ at a stage in its data processing where pollutants carried in cloud water have been returned to the air in preparation for advection and diffusion treatments. CMAQ dry deposits PHg from the lowest layer based on two size modes (Aitken and Accumulation) using the same deposition velocity the model specifies for elemental carbon aerosol in those size modes. It appears that CMAQ may have less efficient dry deposition of its Hg-laden particles than REMSAD and TEAM, especially when CMAQ simulates elemental carbon as being mostly in the accumulation mode.

[48] All three regional-scale models showed an obvious south-to-north gradient in Hg^0 air concentration when using the IC/BC sets based on GEOS-Chem and GRAHM, but no obvious gradient when using the IC/BC set from CTM-Hg. Smaller-scale patterns in Hg^0 air concentration were quite variable between the regional-scale models. Some areas of lower Hg^0 air concentration seem to be associated with simulated chemical oxidation and the combined effect of terrain height and vertical concentration gradients in the IC/BC data. Hg^0 is widely accepted as the least rapidly deposited form of atmospheric Hg. However, Hg^0 can be oxidized to rapidly-depositing forms of Hg, so the dependency of the regional-scale models' simulation of Hg^0 concentrations on the boundary values indicates a need for those boundary values to be accurate.

[49] All of these differences in simulated air concentration for Hg^0, RGM and PHg have implications for the mass balance of Hg fluxes, both between the atmosphere and the surface and between the regional model domain and the rest of the global atmosphere. CMAQ did not simulate dry deposition of Hg^0 nor its evasion from water, soils and vegetation. In effect, CMAQ treated these opposing flux terms as always being in balance. REMSAD did not simulate dry deposition of Hg^0, but it did simulate the evasion of a fraction of deposited RGM and PHg in the form of Hg^0. TEAM simulated dry deposition of Hg^0 and its evasion back to the atmosphere. However, TEAM did not report dry deposition of Hg^0 in its output data because most of it is assumed to be emitted back to the atmosphere. Neither REMSAD nor TEAM reported Hg^0 evasion flux in their output data, so it is not possible to perform a full mass-balance assessment of air/surface exchanges of Hg as simulated by any of these models.

[50] Since Hg^0 deposits slowly and is highly susceptible to surface evasion, the assumption of its net balance of dry

deposition and evasion in the CMAQ simulation may have overlooked an important net source of Hg^0 to the atmosphere. On the other hand, REMSAD showed only about 2 to 3% of its simulated total-Hg deposition was attributable to the Hg^0 evasion it simulated. Unlike the rapidly deposited oxidized Hg species (RGM and PHg), which are emitted mostly from industrial sources, results from all three models showed simulated Hg^0 emissions were largely exported from the model domain by atmospheric transport regardless of whether those Hg^0 emissions were from surface evasion or industrial sources. Therefore the net balance assumption for Hg^0 surface fluxes in CMAQ should have little effect on the strength of the simulated total-Hg deposition flux.

[51] In general, atmospheric concentrations of Hg in air are rarely a direct health concern. It is deposition of atmospheric mercury and subsequent bioaccumulation throughout the terrestrial and aquatic food chain that is of primary concern. The three regional-scale models were significantly different in their simulations of wet and dry depositions of Hg, even when the same IC/BC data were used. Nonetheless, all three regional-scale models showed considerable sensitivity to IC/BC data in their simulated wet and dry deposition patterns.

[52] This study does not determine which of the regional-scale models tested is the most accurate reflection of nature. Due to basic scientific uncertainties regarding the transformation, deposition and recycling of atmospheric mercury, the models applied in this study have many differences in their treatments of these processes. Thus it is difficult, if not impossible, to draw clear conclusions regarding which of these treatments are most responsible for differences in modeling results, even when the same boundary conditions are applied. One clear conclusion we could draw was that each regional-scale model was significantly affected by changes in the lateral boundary conditions applied. Atmospheric mercury transport and deposition depend heavily on both global-scale and regional-scale phenomena. The use of limited-area models for assessment of the emission sources responsible for mercury deposition, whether to specific locations or to entire nations as a whole, requires accurate information about the air concentrations of mercury species at the lateral boundaries. It is the opinion of the authors that we need far more ambient Hg monitoring than is currently being done at the present time.

[53] **Acknowledgments.** A portion of the research presented here was performed under the Memorandum of Understanding between the U.S. Environmental Protection Agency (EPA) and the U.S. Department of Commerce's National Oceanic and Atmospheric Administration (NOAA) and under agreement DW13921548. This work constitutes a contribution to the NOAA Air Quality Program. Although it has been reviewed by EPA and NOAA and approved for publication, it does not necessarily reflect the policies or views of these and the other participating agencies.

References

Ariya, P., et al. (2004), Arctic: A sink for mercury, *Tellus*, *56B*, 397–403.

Bey, I., D. J. Jacob, R. M. Yantosca, J. A. Logan, B. D. Field, A. M. Fiore, Q. B. Li, H. G. Y. Liu, L. J. Mickley, and M. G. Schultz (2001), Global modeling of tropospheric chemistry with assimilated meteorology: Model description and evaluation, *J. Geophys. Res.*, *106*(D19), 23,073–23,095.

Bullock, O. R., and K. A. Brehme (2002), Atmospheric mercury simulation using the CMAQ model: Formulation description and analysis of wet deposition results, *Atmos. Environ.*, *36*, 2135–2146.

Byun, D. W., and K. L. Schere (2006), Review of the governing equations, computational algorithms, and other components of the models-3 Community Multiscale Air Quality (CMAQ) modeling system, *Appl. Mech. Rev.*, *59*, 51–77.

Calvert, J. G., and S. E. Lindberg (2005), Mechanisms of mercury removal by O_3 and OH in the atmosphere, *Atmos. Environ.*, *39*, 3355–3367.

CEC (2004), Preliminary atmospheric emissions inventory of mercury in Mexico, in *Rep. No. 3.2.1.04*, 91 pp., Commission for Environmental Cooperation, Montreal, Canada, 29 June 2004. (Available at http://www.cec.org/files/PDF/POLLUTANTS/MXHg-air-maps_en.pdf)

Dastoor, A. P., and Y. Larocque (2004), Global circulation of atmospheric mercury: A modeling study, *Atmos. Environ.*, *38*, 147–161.

Gery, M. W., G. Z. Whitten, J. P. Killus, and M. C. Dodge (1989), A photochemical kinetics mechanism for urban and regional computer modeling, *J. Geophys. Res.*, *94*(D10), 12,925–12,956.

Grell, G., J. Dudhia, and D. Stauffer (1994), *A Description of the Fifth-Generation Penn State/NCAR Mesoscale Model (MM5), NCAR/TN-398+STR*, 138 pp., National Center for Atmospheric Research, Boulder, Colo.

Gustin, M. S., M. A. Engle, J. Ericksen, S. Lyman, J. Stamenkovic, and M. Xin (2006), Mercury exchange between the atmosphere and low mercury containing substrates, *Appl. Geochem.*, *21*, 1913–1923.

Hansen, J., G. Russel, D. Rind, P. Stone, A. Lacis, S. Lebedeff, R. Ruedy, and L. Travis (1983), Efficient three-dimensional global models for climate studies: Models I and II, *Mon. Weather Rev.*, *111*, 609–662.

Hales, J. M., and S. L. Sutter (1973), Solubility of sulfur dioxide in water at low concentrations, *Atmos. Environ.*, *7*, 997–1001.

Hall, B. (1995), The gas phase oxidation of elemental mercury by ozone, *Water Air Soil Pollut.*, *80*, 301–315.

Horowitz, L. W., S. Walters, D. L. Mauzerall, L. K. Emmons, P. J. Rasch, C. Granier, X. Tie, J.-F. Lamarque, M. G. Schultz, and G. P. Brasseur (2003), A global simulation of tropospheric ozone and related tracers: Description and evaluation of MOZART, version 2, *J. Geophys. Res.*, *108*(D24), 4784, doi:10.1029/2002JD002853.

ICF (2005), User's Guide to the Regional Modeling System for Aerosols and Deposition (REMSAD), in *Rep. No 05-081*, ICF Consulting/SAI, San Francisco, Calif. (Available at http://remsad.saintl.com/documents/remsad_user_guide_v8.00_112305.pdf)

Keeler, G. J., L. Gratz, and K. Al-Wali (2005), Influences on the long-term atmospheric mercury wet deposition at Underhill, Vermont, *Ecotoxicology*, *14*, 71–83.

Lin, C.-J., and S. O. Pehkonen (1999), The chemistry of atmospheric mercury: A review, *Atmos. Environ.*, *33*, 2067–2079.

Lindberg, S. E., and W. J. Stratton (1998), Atmospheric mercury speciation: Concentrations and behavior of reactive gaseous mercury in ambient air, *Environ. Sci. Technol.*, *32*, 49–57.

Lindberg, S. E., R. R. Turner, T. P. Meyers, G. E. Taylor, and W. H. Schroeder (1991), Atmospheric concentration and deposition of Hg to a deciduous forest at Walker Branch Watershed, Tennessee, USA, *Water Air Soil Pollut.*, *56*, 577–597.

Liu, H., D. J. Jacob, I. Bey, and R. Yantosca (2001), Constraints from 210Pb and 7Be on wet deposition and transport in a global three-dimensional chemical tracer model driven by assimilated meteorological fields, *J. Geophys. Res.*, *106*(D11), 12,109–12,128.

Lyman, S. N., M. S. Gustin, E. M. Prestbo, and F. J. Marsik (2007), Estimation of dry deposition of atmospheric mercury in Nevada by direct and indirect methods, *Environ. Sci. Technol.*, *41*, 1970–1976.

Mason, R. P., and G.-R. Sheu (2002), The role of the ocean in the global mercury cycle, *Global Biogeochem. Cycles*, *16*(4), 1093, doi:10.1029/2001GB001440.

Murphy, D. M., P. K. Hudson, D. S. Thomson, P. J. Sheridan, and J. C. Wilson (2006), Observations of mercury-containing aerosols, *Environ. Sci. Technol.*, *40*, 3163–3167.

Pacyna, E. G., J. M. Pacyna, S. Steenhuisen, and S. Wilson (2006), Global anthropogenic mercury emission inventory for 2000, *Atmos. Environ.*, *40*, 4048–4063.

Pacyna, J. M., E. G. Pacyna, F. S. Steenhuisen, and S. Wilson (2003), Mapping 1995 global anthropogenic emissions of mercury, *Atmos. Environ.*, *37*(S1), S109–S117.

Pai, P., P. Karamchandani, and C. Seigneur (1997), Simulation of the regional atmospheric transport and fate of mercury using a comprehensive Eulerian model, *Atmos. Environ.*, *31*, 2717–2732.

Pal, B., and P. A. Ariya (2004), Gas-phase HO-initiated reactions of elemental mercury: Kinetics and product studies, and atmospheric implications, *Environ. Sci. Technol.*, *21*, 5555–5566.

Park, R. J., D. J. Jacob, B. D. Field, R. M. Yantosca, and M. Chin (2004), Natural and transboundary pollution influences on sulfate-nitrate-ammonium aerosols in the United States: Implications for policy, *J. Geophys. Res.*, *109*, D15204, doi:10.1029/2003JD004473.

Pleim, J. E., and A. Xiu (2003), Development of a land surface model. part II: Data assimilation, *J. Appl. Meteorol.*, *42*, 1811–1822.

Poissant, L., M. Pilote, X. Xu, H. Zhang, and C. Beauvais (2004), Atmospheric mercury speciation and deposition in the Bay St. Francois wetlands, *J. Geophys. Res.*, *109*, D11301, doi:10.1029/2003JD004364.

Rea, A. W., S. E. Lindberg, and G. J. Keeler (2000), Assessment of dry deposition and foliar leaching of mercury and selected trace elements based on washed foliar and surrogate surfaces, *Environ. Sci. Technol.*, *34*, 2418–2425.

Ryaboshapko, A., R. Bullock, R. Ebinghaus, I. Ilyin, K. Lohman, J. Munthe, G. Petersen, C. Seigneur, and I. Wangberg (2002), Comparison of mercury chemistry models, *Atmos. Environ.*, *36*, 3881–3898.

Ryaboshapko, A., et al. (2007a), Intercomparison study of atmospheric mercury models. 2: Modelling results vs. long-term observations and comparison of country atmospheric balances, *Sci. Total Environ.*, *377*(2–3), 319–333.

Ryaboshapko, A., et al. (2007b), Intercomparison study of atmospheric mercury models: 1. Comparison of models with short-term measurements, *Sci. Total Environ.*, *376*(1–3), 228–240.

SAI (1999), User's guide to the variable-grid urban airshed model (UAM-V), in *Rep. 02-010*, Systems Applications International, San Rafael, California, USA, October 1999. (Available at http://uamv.saintl.com/documents/uam-v_1.31_user's_guide.pdf)

SAI (2002), An updated photochemical mechanism for modeling urban and regional air quality: Carbon bond, version 5 (CB-V), in *Rep. 02-119*, Systems Applications International, San Rafael, California, USA, 4 December. (Available at http://uamv.saintl.com/members/memos.htm)

Scott, B. C. (1978), Parameterization of sulfate removal by precipitation, *J. Appl. Meteorol.*, *17*, 1375–1389.

Seigneur, C., P. Karamchandani, K. Lohman, K. Vijayaraghavan, and R.-L. Shia (2001), Multiscale modeling of the atmospheric fate and transport of mercury, *J. Geophys. Res.*, *106*(D21), 27,795–27,809.

Seigneur, C., K. Lohman, K. Vijayaraghavan, and R.-L. Shia (2003), Contributions of global and regional sources to mercury deposition in New York State, *Environ. Pollut.*, *123*, 365–373.

Seigneur, C., K. Vijayaraghavan, and K. Lohman (2006), Atmospheric mercury chemistry: Sensitivity of global model simulations to chemical reactions, *J. Geophys. Res.*, *111*, D22306, doi:10.1029/2005JD006780.

Seigneur, C., K. Vijayaraghavan, K. Lohman, P. Karamchandani, and C. Scott (2004), Global source attribution for mercury deposition in the United States, *Environ. Sci. Technol.*, *38*, 555–569.

Selin, N. E., D. J. Jacob, R. J. Park, R. M. Yantosca, S. Strode, L. Jaegle, and D. Jaffe (2007), Chemical cycling and deposition of atmospheric mercury: Global constraints from observations, *J. Geophys. Res.*, *112*, D02308, doi:10.1029/2006JD007450.

Shia, R. L., C. Seigneur, P. Pai, M. Ko, and N. D. Sze (1999), Global simulation of atmospheric mercury concentrations and deposition fluxes, *J. Geophys. Res.*, *104*(D19), 23,747–23,760.

Smolarkiewicz, P. K. (1983), A simple positive definite advection scheme with small implicit diffusion, *Mon. Weather Rev.*, *111*, 479–486.

Sommar, J., K. Gårdfeldt, D. Strömberg, and X. Feng (2001), A kinetic study of the gas-phase reaction between the hydroxyl radical and atomic mercury, *Atmos. Environ.*, *35*, 3049–3054.

Syrakov, D. (2001), Long-term calculation of Hg pollution over south-east Europe, in *Air Pollution Modelling and Its Applications XIV*, edited by S. Grying and F. Schiermeier, pp. 227–235, Kluwer Academic/Plenum Publishers, New York.

US EPA (2005a), Technical support document for the final Clean Air Mercury Rule: Air quality modeling, EPA Office of Air Quality Planning and Standards, Research Triangle Park, North Carolina, March. (Available at http://www.epa.gov/ttn/atw/utility/aqm_oar-2002-0056-6130.pdf)

US EPA (2005b), Emissions inventory and emissions processing for the Clean Air Mercury Rule (CAMR), EPA Office of Air Quality Planning and Standards, Research Triangle Park, North Carolina, March. (Available at http://www.epa.gov/ttn/atw/utility/emiss_inv_oar-2002-0056-6129.pdf)

US EPA (2005c), Clean Air Interstate Rule emission inventory technical support document, EPA Office of Air Quality Planning and Standards, Research Triangle Park, North Carolina, March. (Available at http://www.epa.gov/cair/pdfs/finaltech02.pdf)

Vermette, S., S. Lindberg, and N. Bloom (1995), Field tests for a regional mercury deposition network—sampling design and preliminary test results, *Atmos. Environ.*, *29*, 1247–1251.

Wang, Y., D. J. Jacob, and J. A. Logan (1998), Global simulation of tropospheric O3-NOx-hydrocarbon chemistry: 1. Model formulation, *J. Geophys. Res.*, *103*(D9), 10,713–10,726.

Wesely, M. L. (1989), Parameterization of surface resistances to gaseous dry deposition in regional-scale numerical models, *Atmos. Environ.*, *23*, 1293–1304.

Xiu, A., and J. E. Pleim (2001), Development of a land surface model. part I: Application in a mesoscale meteorological model, *J. Appl. Meteorol.*, *40*, 192–209.

Zhang, L., J. R. Brook, and R. Vet (2003), A revised parameterization for gaseous dry deposition in air-quality models, *Atmos. Chem. Phys. Discuss.*, *3*, 1777–1804.

Zhang, L., S. Gong, J. Padro, and L. Barrie (2001), A size-segregated particle dry deposition scheme for an atmospheric aerosol module, *Atmos. Environ.*, *35*, 549–560.

D. Atkinson, Office of Water, U.S. Environmental Protection Agency, 1200 Pennsylvania Avenue NW, Mail Code 4503-T, Washington, DC 20004, USA.

T. Braverman, Office of Air Quality Planning and Standards, U.S. Environmental Protection Agency, 109 T.W. Alexander Drive, Mail Drop C439-01, Research Triangle Park, NC 27711, USA.

O. R. Bullock Jr., National Exposure Research Laboratory, U.S. Environmental Protection Agency, Mail Drop E243-03, Research Triangle Park, NC 27711, USA. (bullock.russell@ epa.gov)

K. Civerolo, J.-Y. Ku, and G. Sistla, Division of Air Resources, New York State Department of Environmental Conservation, 625 Broadway, Albany, NY 12233-3259, USA.

A. Dastoor and D. Davignon, Air Quality Research Division, Environment Canada, 2121 Trans Canada Highway, 5th floor, Dorval, QC, Canada H9P 1J3.

K. Lohman, C. Seigneur, and K. Vijayaraghavan, Air Quality Division, Atmospheric and Environmental Research, Inc., 2682 Bishop Drive, Suite 120, San Ramon, CA 94583, USA.

T. C. Myers, ICF International, 101 Lucas Valley Road, Suite 260, San Rafael, CA 94903, USA.

R. J. Park, School of Earth and Environmental Sciences, Seoul National University, 599 Gwanangno, Gwanakgu, Seoul 151-742, South Korea.

N. E. Selin, Massachusetts Institute of Technology, Department of Earth, Atmospheric and Planetary Sciences, 77 Massachusetts Avenue, Cambridge, MA 02139-4307, USA.